Galaxies in 3D across the Universe
Proceedings IAU Symposium No. 309, 2014
B. L. Ziegler, F. Combes, H. Dannerbauer, M. Verdugo, eds.

DOI: 10.1017/X000000000000000X

Disk Galaxies in the Magneticum Pathfinder Simulations

Rhea-Silvia Remus[1], Klaus Dolag[1,2], Lisa K. Bachmann[1], Alexander M. Beck[1,2], Andreas Burkert[1,3], Michaela Hirschmann[4], & Adelheid Teklu[1]

[1]Universitäts-Sternwarte München, Scheinerstr. 1, D-81679 München, Germany
[2]MPI for Astrophysics, Karl-Schwarzschild Strasse 1, D-85748 Garching, Germany
[3]MPI for Extraterrestrial Physics, Giessenbachstrasse 1, D-85748 Garching, Germany
[4]Institut d'Astrophysique de Paris, UPMC-CNRS, UMR7095, Boulevard Aragon, F-75014 Paris, France
email: rhea@usm.lmu.de

Abstract. We present *Magneticum Pathfinder*, a new set of hydrodynamical cosmological simulations covering a large range of cosmological scales. Among the important physical processes included in the simulations are the chemical and thermodynamical evolution of the diffuse gas as well as the evolution of stars and black holes and the corresponding feedback channels. In the high resolution boxes aimed at studies of galaxy formation and evolution, populations of both disk and spheroidal galaxies are self-consistently reproduced. These galaxy populations match the observed stellar mass function and show the same trends for disks and spheroids in the mass–size relation as observations from the SDSS. Additionally, we demonstrate that the simulated galaxies successfully reproduce the observed specific angular-momentum–mass relations for the two different morphological types of galaxies. In summary, the *Magneticum Pathfinder* simulations are a valuable tool for studying the assembly of cosmic and galactic structures in the universe.

1. Introduction

The observational properties of galaxies have been studied in a multitude of surveys, but until recently corresponding simulations including baryonic physics were limited to isolated or merging systems and cosmological zoom-in simulations of individual galaxies selected from larger cosmological boxes of low resolution. With increasing computational power and improved models of the physics that drive the evolution of baryonic structures it has now become possible to simulate large cosmological volumes with full baryonic treatment, providing sufficiently large samples of galaxies formed within the cosmological ΛCDM model to study the statistical properties of galaxies and compare them with observations. These new simulations will significantly improve our understanding of the formation and evolution of all types of galaxies, their dynamical properties, and the changes of morphology across cosmic time. Especially, they will shed light on the two dominant processes of galaxy formation, namely mergers and secular evolution. We present one such set of new cosmological simulations, called *Magneticum Pathfinder*, and show first results on the simulated galaxy properties in comparison to observations.

2. The Magneticum Pathfinder Simulations

The Magneticum Pathfinder simulations (Dolag et al., in prep.) are a set of hydrodynamical cosmological boxes with volumes ranging from $(896\ \mathrm{Mpc}/h)^3$ to $(18\ \mathrm{Mpc}/h)^3$ and resolutions of $m_{\mathrm{Gas}} = 2.6 \cdot 10^9 M_\odot/h$ up to $m_{\mathrm{Gas}} = 3.9 \cdot 10^5 M_\odot/h$, performed with a modified version of GADGET (Springel 2005). They include radiative cooling, star formation

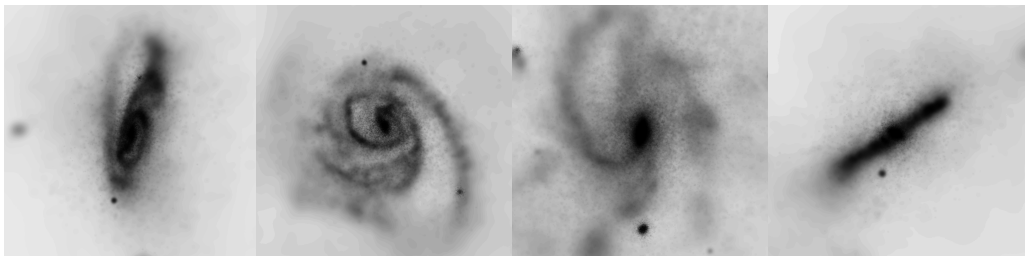

Figure 1. Examples of disk galaxies from the Magneticum Pathfinder Simulations.

and kinetic winds following Springel & Hernquist (2003), stellar evolution and metal enrichment according to Tornatore et al. (2007) and Wiersma et al. (2009), and black hole evolution and feedback of Springel et al. (2005), Fabjan et al. (2010) and Hirschmann et al. (2014). Furthermore, we implemented several improvements for smoothed particle hydrodynamics that more accurately treat turbulence and viscosity and result in a better modeling of galaxies (Dolag et al. 2005, Beck et al., in prep., for details). Additionally, we include thermal conduction according to Dolag et al. (2004). We adopt a WMAP7 (Komatsu et al. 2011) ΛCDM cosmology with $h = 0.704$, $\Omega_m = 0.272$ and $\Lambda = 0.728$, and use SUBFIND (Springel et al. 2001, Dolag et al. 2009) to identify and extract structures from galaxy clusters down to galaxies.

3. Galaxies in the Magneticum Pathfinder Simulations

To study galactic dynamics in detail, high resolution is required. Therefore, we use the largest box with sufficient resolution (box length of 48 Mpc/h and resolution of $m_{\rm DM} = 3.6 \cdot 10^7 M_\odot/h$, $m_{\rm Gas} \approx 7.3 \cdot 10^6 M_\odot/h$, and slightly smaller stellar mass) for reproducing the observed diversity of morphologies and kinematic properties with adequate statistics. We follow $(2 \cdot 576)^3$ particles, employing a softening length of $\epsilon_{\rm DM,Gas} = 1.4$ kpc/h for dark matter and gas and $\epsilon_* = 0.7$ kpc/h for stars. The box contains 621 halos down to a mass of $5 \cdot 10^{11} M_\odot/h$, of which five are small clusters and approximately 40 are groups above $10^{13} M_\odot/h$ at redshift $z = 0$. Thus, we can study the dynamics and properties of galaxies down to normal Milky Way type galaxies; however, our resolution is insufficient

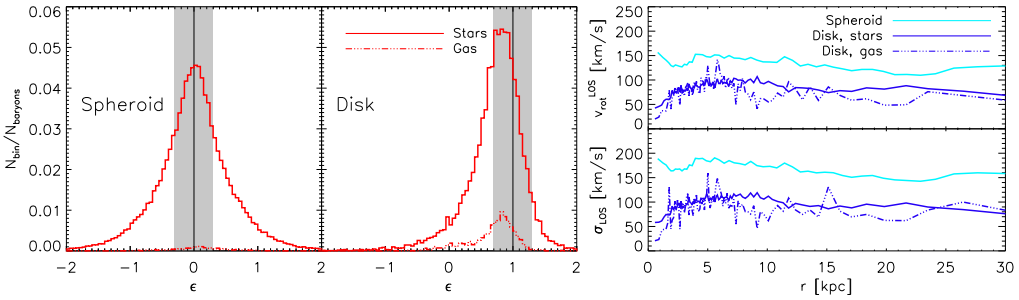

Figure 2. *Left:* Distribution of the circularity ϵ of a spheroidal (left) and a disk galaxy (right) for stars (solid red) and gas (dash-dotted red) within $0.1R_{\rm vir}$, normalized to the total stellar and gas mass of the galaxy. Gray shaded areas mark the selection criterion for spheroid (left) and disk (right) galaxies used in this work. *Right:* Line-of-sight (LOS) velocity (upper) and LOS velocity dispersion (lower panel) versus radius for the stellar component of the spheroid (cyan) and the disk (blue) galaxy and the gas component of the disk galaxy (dashed blue). The spheroidal clearly has a higher dispersion relative to its rotation velocity, while for the disk both the stellar and gas component are in very good agreement, as expected from observations.

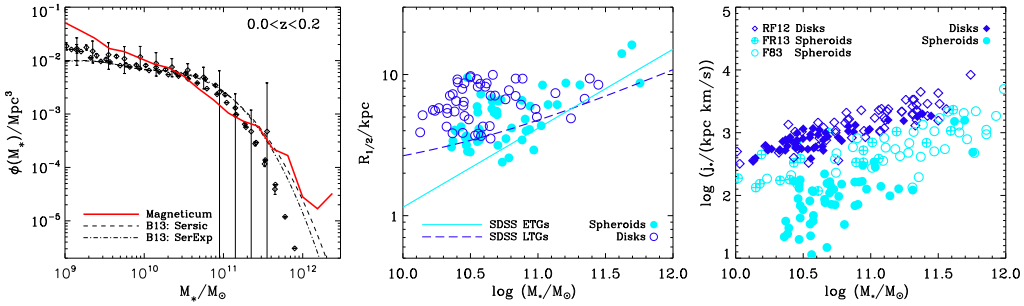

Figure 3. *Left:* Stellar mass functions for $z < 0.2$ in our simulation (solid line) compared to observations (diamonds, data points from Cole et al. 2001, Bell et al. 2003, Panter et al. 2004 and Pérez-González et al. 2008). For high stellar masses observational estimations are uncertain as discussed in Bernardi et al. 2013 (B13, using a Sérsic model (dashed) and a Sérsic-bulge-plus-exponential-disk model (dash-dotted line)). *Middle:* Mass–size relation of the simulated disks (blue open circles) and spheroids (cyan filled circles). The dashed blue and solid cyan lines represent the mean size as function of mass from Shen et al. 2003 for SDSS early-type and late-type galaxies. *Right:* Specific angular momentum of the stellar component of the simulated disks (blue filled diamonds) and spheroids (cyan filled circles) as function of the stellar mass. Open symbols represent the observations of disk galaxies from Romanowsky & Fall 2012 (RF12, blue diamonds) and for ellipticals from Fall & Romanowsky 2013 (FR13, cyan plussed circles) and Fall 1983 (F83, cyan open circles).

to properly resolve dwarf galaxies. Fig. 1 shows some typical disk galaxies formed in this simulation.

3.1. *The Classification of Galaxies*

We successfully reproduce a population of disk as well as spheroidal galaxies due to the improvements in the numerical methods as well as the included prescriptions of physical processes. To distinguish the populations and classify the galaxies, we use a procedure similar to Scannapieco et al. (2008): we align each galaxy along its principal axis of inertia of the stars within $0.1R_{\rm vir}$ and subsequently classify it according to the circularity parameter $\epsilon = j_z/j_{\rm circ}$, where j_z is the specific angular momentum of each particle with respect to the z-axis and $j_{\rm circ}$ is the specific angular momentum expected for a circular orbit. We classify a galaxy as spheroidal if more than 40% of both stellar and gas particles lie within $-0.3 \leqslant \epsilon \leqslant 0.3$, and as disk if more than 40% of its gas and more than 30% of its stellar particles are within $0.7 \leqslant \epsilon \leqslant 1.3$. Fig. 2 shows the distribution of ϵ for a spheroid and a disk (left panel). We identify 51 clearly rotationally supported disks and 51 clearly dispersion-dominated spheroids from our sample of 621 galaxies at $z = 0$. Our criterion is fairly strict, excluding systems like S0 galaxies, spheroids with gas disks, merging systems and disk galaxies with bar-like structures from the classification.

3.2. *Population Characteristics*

The stellar mass function for all central galaxies (independent of their classification type) is shown in Fig. 3 (left panel). A similar analysis for other boxes of the Magneticum simulations has been shown by Hirschmann et al. (2014) and Bachmann et al. (2014). Our simulation is in good agreement with the observations, apart from an overestimate at the low-mass end, where the simulation does not resolve the feedback associated with black holes. Another important characteristic of galaxy properties is the mass–size relation: for the same mass, spheroidal galaxies are more compact than their disky counterparts. As shown in the middle panel of Fig. 3, our disks and spheroids show the same behaviour as the observations, even though our calculation of the stellar half-mass radius is only a crude

approximation to the observed half-light radius determined from Sérsic fits (Shen et al. 2003). More details on the dynamical properties of our sample of galaxies are presented by Remus et al. (in prep.). The right panel of Fig. 3 shows the specific angular-momentum–mass relation of the stars in our disk and spheroidal galaxies compared to observations from Fall (1983), Romanowsky & Fall (2012) and Fall & Romanowsky (2013). Again, our simulated galaxies are in excellent agreement with the observations, showing the clear distinction between the specific stellar angular momentum of disks and spheroids, which is discussed in more detail by Teklu et al. (in prep).

4. Conclusions

The Magneticum simulations can successfully reproduce disk galaxies as well as spheroids, with enough resolution to study dynamical properties of those galaxies. We demonstrated that Magneticum galaxies match the observed properties of present-day disk and spheroid galaxies, such as the stellar mass function and the mass–size and angular-momentum–mass relations. This renders possible a statistical approach to the different evolution mechanisms of both disks and spheroidals, which will be done in several forthcoming studies.

Acknowledgements

The Magneticum team acknowledges support from the DFG Excellence Cluster Universe, the SFB-Transregio TR33, the Computational Center C2PAP, and the Leibniz-Rechenzentrum via projects pr86re and pr83li.

References

Bachmann, L. K., *et al.* 2014, arXiv:1409.3221
Bell, E. F., McIntosh, D. H., Katz, N., & Weinberg, M. D. 2003, ApJS, 149, 289
Bernardi, M., *et al.* 2013, MNRAS, 436, 697
Cole, S., *et al.* 2001, MNRAS, 326, 255
Dolag, K., Jubelgas, M., Springel, V., Borgani, S., & Rasia, E. 2004, ApJ, 606, L97
Dolag, K., Vazza, F., Brunetti, G., & Tormen, G. 2005, MNRAS, 364, 753
Dolag, K., Borgani, S., Murante, G., & Springel, V. 2009, MNRAS, 399, 497
Fabjan, D., *et al.* 2010, MNRAS, 401, 1670
Fall, S. M. 1983, in IAU Symposium, Vol. 100, Internal Kinematics and Dynamics of Galaxies, ed. E. Athanassoula, 391–398
Fall, S. M. & Romanowsky, A. J. 2013, ApJ, 769, L26
Hirschmann, M., *et al.* 2014, MNRAS, 442, 2304
Komatsu, E., *et al.* 2011, ApJS, 192, 18
Panter, B., Heavens, A. F., & Jimenez, R. 2004, MNRAS, 355, 764
Pérez-González, P. G., *et al.* 2008, ApJ, 675, 234
Romanowsky, A. J. & Fall, S. M. 2012, ApJS, 203, 17
Scannapieco, C., *et al.* 2008, MNRAS, 389, 1137
Shen, S., *et al.* 2003, MNRAS, 343, 978
Springel, V. 2005, MNRAS, 364, 1105
Springel, V., Di Matteo, T., & Hernquist, L. 2005, MNRAS, 361, 776
Springel, V. & Hernquist, L. 2003, MNRAS, 339, 289
Springel, V., White, S. D. M., Tormen, G., & Kauffmann, G. 2001, MNRAS, 328, 726
Tornatore, L., Borgani, S., Dolag, K., & Matteucci, F. 2007, MNRAS, 382, 1050
Wiersma, R. P. C., Schaye, J., & Smith, B. D. 2009, MNRAS, 393, 99